Fatigue crack growth prediction of band overloaded 7075-T651 aluminium alloy by Exponential model and Gamma model

A thesis submitted in partial fulfilment of the requirements for award of the degree of

Master of Technology (Research)

By

S.V. Abhinay

(Roll No. 612MM3008)

Under the supervision of

Prof. B.B.Verma
Department of Metallurgical and Materials Engineering
National Institute of Technology
Rourkela-769008

Prof. P.K. Ray
Department of Mechanical Engineering
National Institute of Technology
Rourkela - 769008

Department of Metallurgical and Materials Engineering
National Institute of Technology Rourkela- 769008
Odisha (INDIA)

Department of Metallurgical and Materials Engineering
National Institute of Technology Rourkela
Rourkela-769008, Odisha, India

This is to certify that the thesis entitled, **"Fatigue crack growth prediction of band overloaded 7075-T651 aluminium alloy by Exponential model and Gamma model"** submitted by **Mr. S. V. Abhinay** in partial fulfillment of the requirements for the award of Master of Technology (Research) Degree in **Metallurgical & Materials Engineering** at National Institute of Technology, Rourkela, Odisha (INDIA) is an authentic work carried out by him under our supervision and guidance. To the best of our knowledge, the matter embodied in the thesis has not been submitted to any other University/ Institute for the award of any degree or diploma.

Prof. B.B.Verma

Department of Metallurgical and Materials Engineering

National Institute of Technology

Rourkela-769008

Prof. P.K. Ray

Department of Mechanical Engineering

National Institute of Technology

Rourkela - 769008

Date:

Place:

Acknowledgement

It is a privilege for me to express my profound gratitude and indebtedness to my supervisors Prof. B.B. Verma, Metallurgical & Materials Engineering Department, Prof. P. K. Ray Department of Mechanical Engineering, National Institute of Technology Rourkela. Without their efforts and guidance this work could not have been possible. They have guided me at all stages during this research work. I will cherish all the moments of enlightenment they have shared with me.

My sincere thanks to Prof. Sunil Kumar Sarangi, Director, N.I.T, Rourkela and Prof. S. C. Mishra, HOD (MM) for granting permission to use the facilities available in the institute.

I am thankful to my seniors and friends Mr. Vaneshwar Kumar Sahu, Mr. Ajit Kumar, Mr. Naresh Kumar, Mr. Omprakash Tenduwe, Mr. Premendra Mani Pradhan and Mr. Amar Joshi for their help and support during my research work. I am also thankful to Mr. S. Hembram, Mr. Rajesh Patnaik, Mr. S. Pradhan Metallurgical & Materials Engineering Department, National Institute of Technology Rourkela for their technical guidance in conducting various experimental studies during the research work.

I thank my parents for always being there for me. With their help and encouragement I was able to undertake this work. I would like to thank all my friends for making my stay at NIT Rourkela a memorable journey of my life.

S.V. Abhinay

Date:

Place:

Abstract

Fatigue is the most important cause of mechanical failure of engineering structures and components. In majority of the cases the stress amplitude does not remain constant and undergoes variation with time. Fatigue crack growth in structures/components subjected to variable amplitude loading is complex. Fatigue crack growth under multiple overloads is the building block to study the effect of variable amplitude loads.

In the present investigation an attempt has been made to study the effect of single overload and band overloads on fatigue crack growth behaviour of 7075-T651 aluminium alloy at room temperature. The tests were conducted on compact tension specimens. Single overload and band overloads were introduced during constant amplitude fatigue loading in mode-I condition. The maximum retardation occurred on introduction of band overload consisting 7 overload cycles.

It is known that the introduction of overload cycles alters the crack growth behaviour. In the present work an "Exponential model" and a "Gamma model" have been developed to predict crack growth rate and fatigue life of specimens subjected to overload cycles. The predicted results by both the models are found in good agreement with the experimental data.

Keywords: Fatigue crack growth rate, Overload, Band-overload, 7075 T651 aluminium alloy, Exponential model, Gamma model.

Contents Page No.

List of Figures

List of Tables

Nomenclature

a_o	Initial crack length , mm
a_i	Crack length at i^{th} step, mm
a_f	Final crack length, mm
a_j	Crack length at j^{th} step, mm
a_n	Notch length, mm
a_{ol}	Crack length at overload point, mm
(a/W)	Ratio of crack length to width of specimen
$(a/W)_{ol}$	Ratio of crack length to width of specimen at overload point
B	Specimen thickness, mm
CT	Compact tension
da/dN	Crack growth rate, mm/cycle
E_m	Modulus of Elasticity
f	Frequency, Hz
f_{ol}	Frequency at overload , Hz
K	Stress intensity factor, mpa√m
K_c	Plane strain fracture toughness
K_{max}	Maximum stress intensity factor, mpa√m
K_{min}	Minimum stress intensity factor, mpa√m
l	Dimensionless parameter
m	Specific crack growth rate
N	Number of cycles
n	Number of overload cycles
W	Width of specimen, mm
σ_{max}	Maximum stress, kN
σ_{min}	Minimum stress, kN

Chapter-1

INTRODUCTION

1. INTRODUCTION

1.1. Background

Fatigue is the most important cause of mechanical failure of engineering structures and components. In majority of the cases the stress amplitude does not remain constant and undergoes variation with time. Fatigue crack growth in structures/ components subjected to variable amplitude loading is complex. Fatigue crack growth under single or multiple overloads is the building block to study the effect of variable amplitude loads. An aircraft experiences overload cycles during gust. Ships experience high amplitude stress during tide. The occurrence of high amplitude load is also common in offshore structures and earth movers. It is known that overload application induces crack growth retardation resulting enhancement of fatigue life [1-6].

Many fatigue life prediction models have been proposed based on the loading conditions [7-13]. Most of these models are formulated using the loading variables, the crack growth rate and fracture mechanics parameters. After formulating the equation, life is estimated using cycle by cycle integration. The whole process becomes complicated because of the involvement of robust numerical integration scheme.

The main objectives of current work are to study the effect of overload (spike and band) on fatigue crack growth behaviour and formulate models to predict residual fatigue life without any complex integration scheme. This has been achieved by adopting a modified exponential

model and using a gamma function. The models are found to be in good agreements with the experimental post overload behaviour.

1.2 Plan of work

The work plan of present research work can be visualized from flow chart presented in Fig. 1.1.

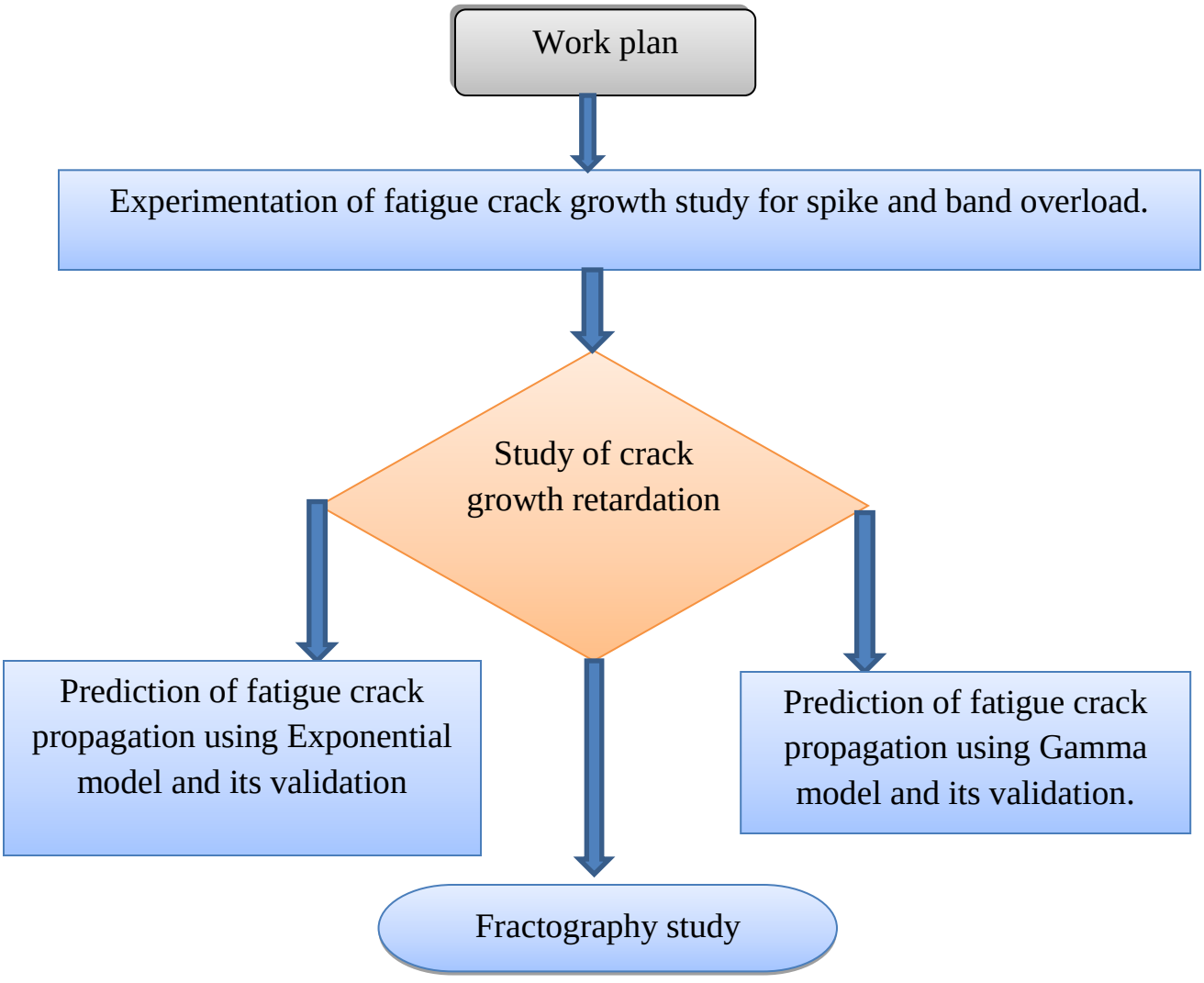

Fig.1.1- Work plan of present investigation

1.3 Objective

The objectives of present examination are-

- To study the effect of single overload and band overload application on fatigue life of 7075-T651aluminium alloy at room temperature.
- To predict fatigue crack propagation rate and residual life using exponential model and gamma model.

1.4 Structure of thesis

The thesis comprises abstract of the investigation, 8 chapters and a list of referred literature. Chapter 1 and Chapter 2 deal with an introduction and a brief review of literature. In Chapter 3 the details of materials and experimentation procedures are presented. The experimental results and analysis of experimental observations are discussed in Chapter 4. Chapter 5 deals with development of an exponential model and its validation using experimental results. Chapter 6 deals with development of a gamma model and its validation using a set experimental data. Comparisons of predicted results are highlighted in Chapter 7. Chapter 8 describes the conclusion and future work to be done.

Chapter 2

LITERATURE REVIEW

2.1Fatigue and its fatigue failure- mechanism

Metal fatigue is defined as a process which causes premature failure of engineering parts or component head to repeat reversed or cyclic loading. These structures are found to fail, when the actual maximum stress is below the actual ultimate strength and in few cases even less than the actual yield strength [14]. Fatigue is estimated to cause operational service failures of metallic components and structures such as in bridges, machine components, aircraft, etc. subjected to variable or constant fluctuating load or cyclic stresses. Since fatigue crack growth is driven dominatingly by crack tip plasticity and plastic strains (intrinsically irreversible), changes in the load patterns invariably result in transient effects which influences fatigue crack growth rates and hence the fatigue life.

2.1.1 Stages of fatigue crack growth

Fatigue proceeds in three different stages as:

1. Crack initiation

Region–I:

- Early development of damage.
- Difficulty in defining crack size (dislocation, micro-crack, porosity etc.)

2. Crack propagation

Region–II- crack growth

- Deepening of initial crack on shear planes.
- Crack can first be observed in an engineering sense.
- Precise crack growth on planes normal to maximum tensile stress.
- Crack growth can be observed.

3. Final catastrophic failure

- Ultimate failure of materials.

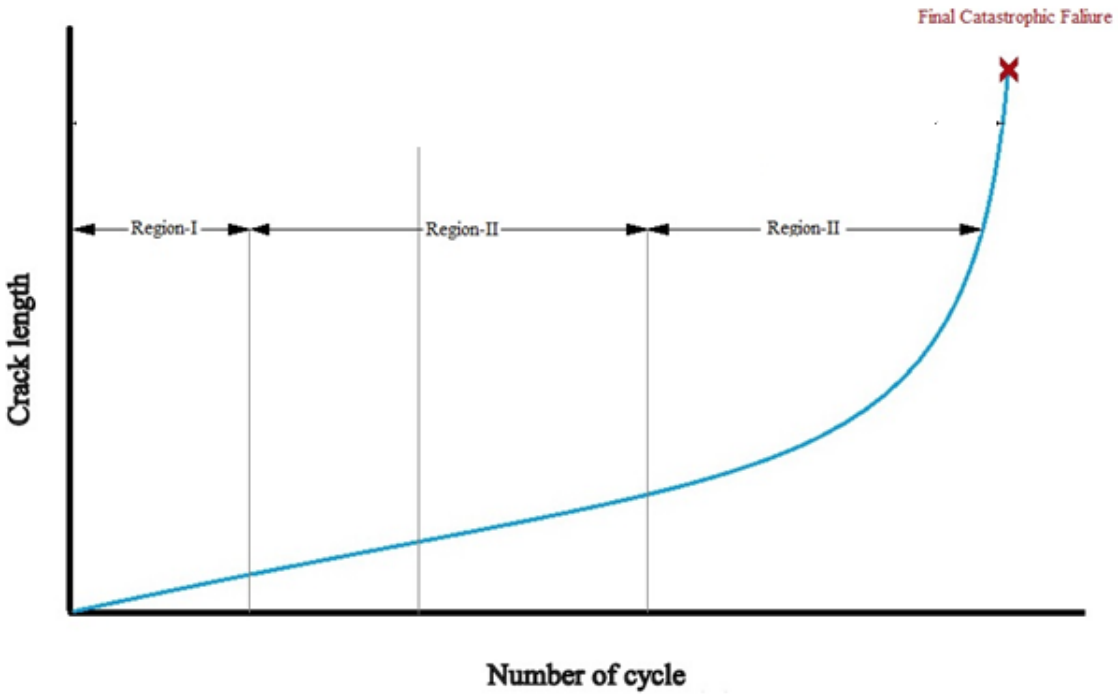

Fig. 2.1- Schematic relation between crack initiation, propagation and catastrophic failure.

2.1.2 The macro mechanism of fatigue failure

The mechanism of fatigue failure is explained as-

1. Crack initiation -It occurs in the areas of localized stress concentration such as notches holes, slots, key ways. Also cracks may initiate at surface, and geometrical discontinuities, and sites of existing cracks and inclusions.
2. Incremental crack propagation - By increasing the stress levels further, propagation of fatigue cracks takes place at the grains or along the grain boundaries, by slow increment of crack size.
3. Final catastrophic failure - As the area happens to become too deficient to resist the induced stresses sudden fracture results in the structures or machine components. At the final stage of fatigue, material is conclusively failed.

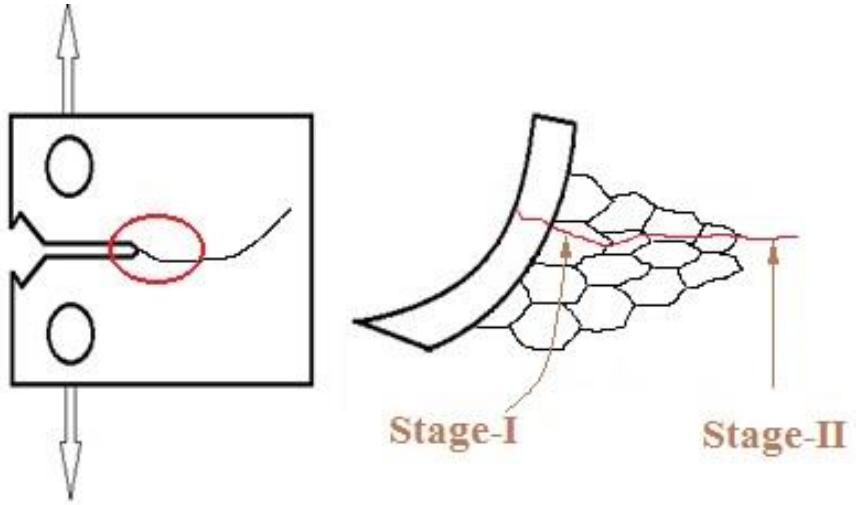

Fig. 2.2-Behaviour of fatigue crack growth in a CT specimen

2.2 Fatigue crack growth

By the application of fracture mechanics approach, prediction of the number of cycles for a crack to reach some definite length can be done. The load ratio effects on the behaviour of fatigue crack growth rate have been reported for some standard geometric specimens [15]. Behavior of fatigue crack growth mostly depends on the state of stress at the notch tip zone, the geometry, and shape of the, notch and loading parameters etc.

Proper and realistic prediction of fatigue crack growth for safe-life or fail-safe design approach is mostly concerned in aircraft industry. Accordingly by having good knowledge about the material crack growth behaviour and attributes with standard examinations, a cracked structure or machine part may be preceded in service with a broadened life [16].

2.3 Regions of crack growth rate curve

It is known that for nearly all metallic structural materials the da/dN versus ΔK is sigmoidal and the curve clearly shows three distinct regions of crack growth rate associated with the cyclic stress intensity range ΔK. At the lower end starting from a ΔK threshold (ΔK_{th}) below which the crack growth rate is near zero, the crack is nonpropagating (crack simply opens and closes without any forward movement). The existence of this threshold is analogous to the fatigue limit of ferrous materials in *S-N* fatigue. In this region, at least in principle, the fatigue crack growth rate is negligible for an unlimited number of cycles. Physically this means that as the threshold is approached, the average crack growth rate approaches the limiting value of one inter atomic spacing per cycle. Therefore, the fatigue crack threshold is an important design

parameter particularly in applications involving rotating shafts subjected to low stresses and high-frequency fatigue where any crack extension during service cannot be permitted.

The intermediate linear region can be represented by simple power law relationship

$$da/dN = C\,(\Delta K)^m$$

Where m and C are material constants and $\Delta K = K_{max} - K_{min}$.

The graph between log (da/dN) vs. log (ΔK) is presented in Fig.2.3. This plot can be divided in to three regions.

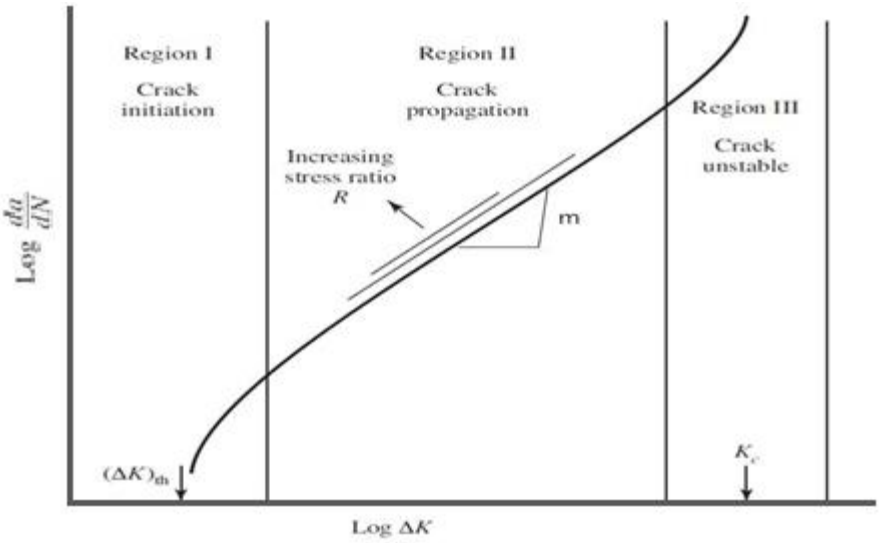

Fig. 2.3- Different regions of crack growth rate curve

Region-I*:* This region is the crack initiation zone in which log (da/dN) increase asymptotically with log (ΔK). This is fatigue threshold zone where the ΔK is value is not enough to propagate a crack. Crack initiation do not take place until ΔK reaches certain threshold value known to be ΔK_{th}, below which the growth in da/dN is too low that cannot be experimentally measured.

Region II: It is also called as crack propagation or Paris regime in which crack growth rate is followed a linear variation with respect to increasing in log ΔK. Stable crack growth is observed in this region.

Region III: Fast fatigue crack growth rates are observed in this region.

2.4 Literature on effects of overload and band overload on fatigue crack growth and modeling.

Single overload application decrease the fatigue crack growth rate and increase the delay crack length by the formation of a larger plastic zone [17] shown in Fig. 2.4 **.** An overload is a pulse or a set of pulses of higher amplitude interspersed on a constant amplitude fatigue loading, shown in Fig. 2.5 and Fig. 2.6. Retardation of crack propagation takes place after the overload pulse [18, 19]. In second region of fatigue crack growth, overloads can have a very significant effect on fatigue life. High crack tip strain induces a large zone of plastic deformation ahead of the crack tip during the overload. During unloading, elastic material tries to recover its unique state, however the plastic zone can't recapture the original state and this leads to the development of compressive residual stresses in the surrounding region of crack tip. This retardation effect is presented in Fig. 2.7. The number of delay cycles N_d refers to number of load cycles required to restore the pre-overload crack growth minus the number of cycles needed to reach the same crack length without an overload (constant amplitude loading). The affected crack length or retarded zone length a_d refers to the crack length over which the retardation occurred due to application of overload. Schematic representation of delay cycles N_d and retarded crack length a_d following overload is represented in Fig. 2.8.

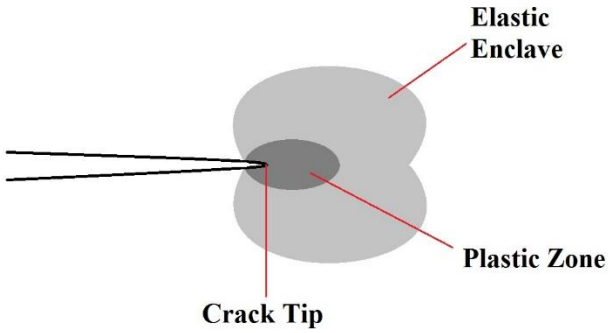

Fig. 2.4 - Induced plastic volumetric expansion zone at the front of crack tip during a tensile overload .

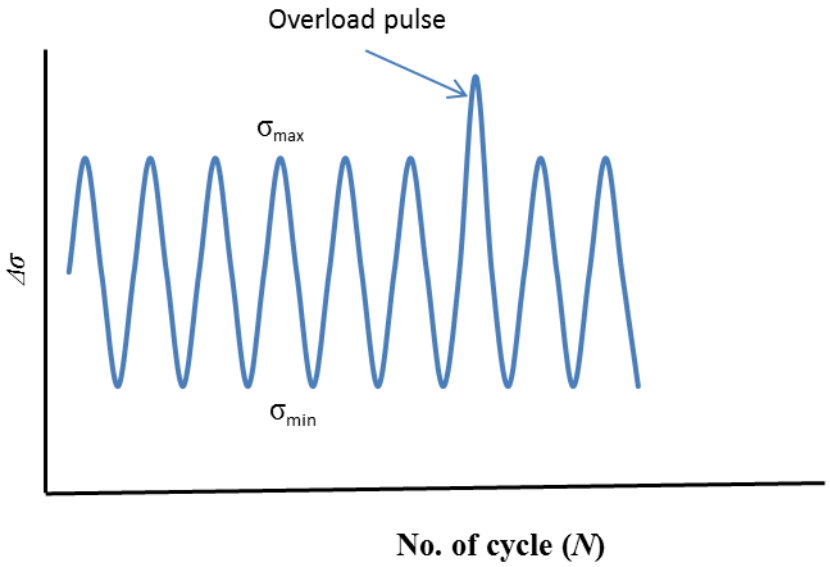

Fig. 2.5- Single overload pulse on the constant amplitude fatigue load cycle.

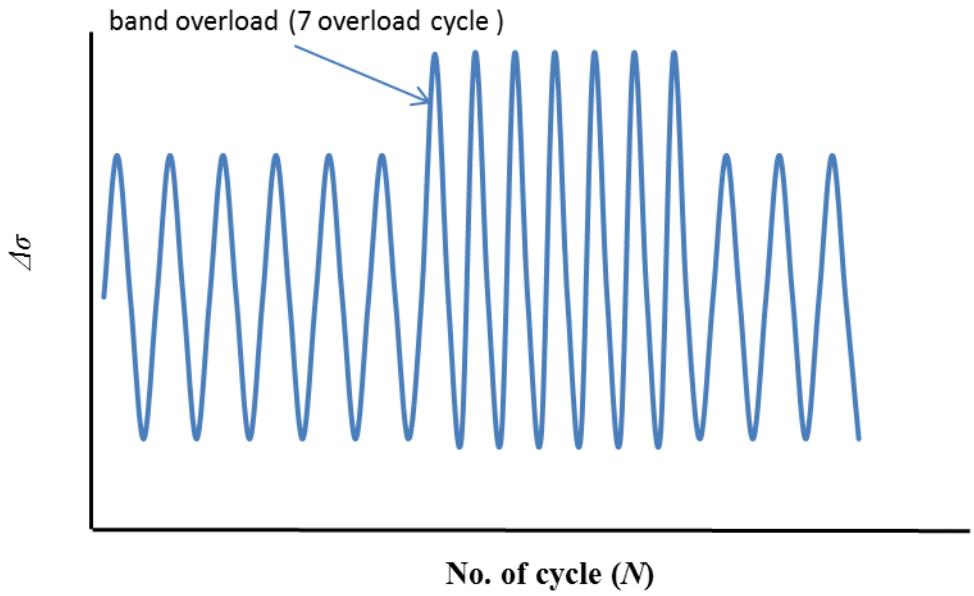

Fig.2.6 -Seven overload band on the constant amplitude fatigue load cycle.

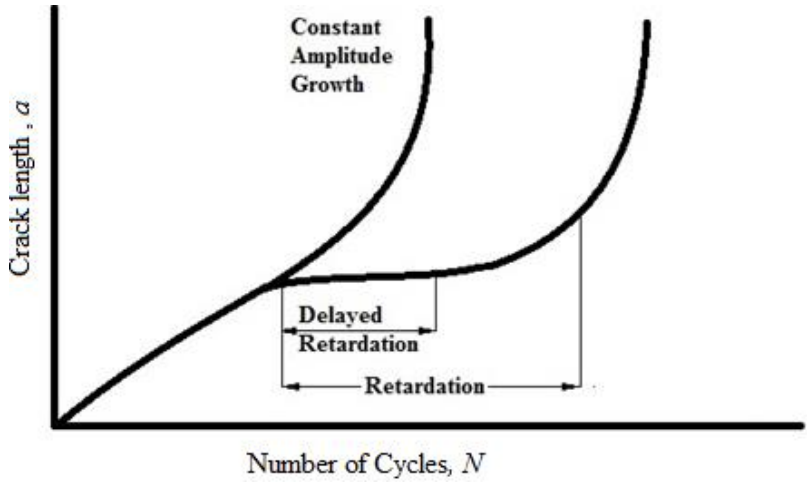

Fig. 2.7- Retardation in fatigue crack growth in *a*-*N* plot by overload and band overload application.

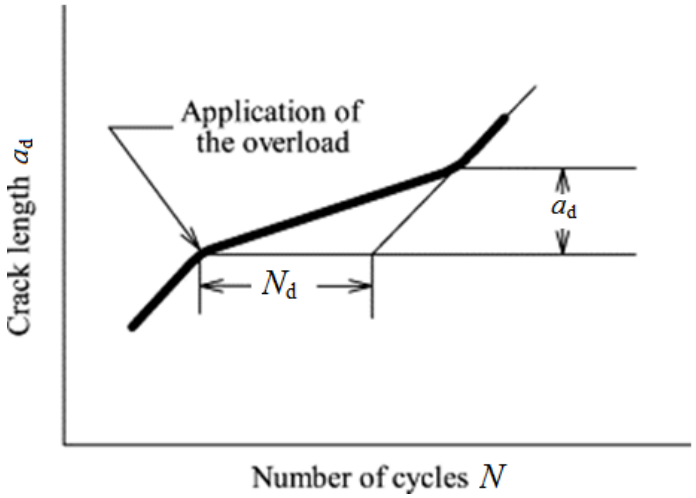

Fig. 2.8 -Schematic representation of delay cycles N_d and retarded crack length a_d following overload.

The application of single overload of moderate stress level is known to retard a growing fatigue crack due to development of large monotonic plastic zone at the crack tip enclosed in an elastic enclave [3, 4, 16, and 21]. This retardation is proportional to the relative decrease in the size of the monotonic plastic zone attending the crack tip. Retardation after the imposition of overloads is known to be operative through a distance that is proportional to the extent of the overload plastic zone [3, 4]. Crack closure experiments on 6061-T6 Al-alloy for various bands of overloads were studied [22]. The sequence is almost constant amplitude loading with periodically inserted multiple overloads, which subsequently cause noticeable crack growth delay.

Application of overload results in sharp edge of crack tip to become blunted. This reduces severe stress concentrations that are present at sharp edge of crack tip [23]. Several investigators [24, 25, and 26] observed that magnitude of cyclic overload results in retardation or acceleration in fatigue crack growth rate. The retardation effect on fatigue crack growth due to variable amplitude loading was studied in 7075 T6511 aluminum alloy by Corbly and

Packman [11]. It has been observed that the amount of retardation depends on the number of stress applications at the peak stress intensity, relative amplitudes of the peak stress intensity and the number of fatigue cycles at the lower stress intensity level after the last peak stress is applied.

Several models have been proposed to explain the phenomenon of crack growth delay. In general, these models attribute the delayed behavior to crack-tip blunting, residual stresses [10, 27] crack closure [28], or a combination of these mechanisms. A crack tip blunting model advocates that high tensile load cycles cause crack tip blunting, which in turn causes retardation in fatigue crack growth at the lower cyclic load fluctuations until the crack is re-sharpened. Residual stress model suggests that on application of a high overload cycle residual compressive stresses generate in the locality of the crack tip that reduce the rate of fatigue crack growth. The crack closure model postulates that the delay in fatigue crack growth is caused by the formation of a zone of residual tensile deformation left in the wake of a propagating crack that causes the crack to remain closed during a portion of the applied tensile load cycle. It is generally considered that most widely used fatigue crack growth equation is Paris-Erdogan relation [29], from which most of differential form of fatigue cracks growth models is proposed. According to literature [30, 31], its limitations has been discussed. An exponential model has been formulated by Mohanty.*et.al* to estimate fatigue life under different loading conditions [32-34]. Significance of specific crack growth and its dependence has been discussed in the above model. Significance of specific crack growth and its dependence has been discussed in the above model. An exponential model has been proposed for the prediction of crack growth behavior and various retardation factors in case of single overload spike induced constant amplitude loading condition. The predicted results are

compared with the experimental data and the values obtained from Wheeler's retardation model [32]. Exponential model of the form $a = a_0 e^{mN}$ has effectively used to determine the retardation parameters a_d and N_d [33]. 'Extended Exponential Model' of the form $aj=a_i e^{m_{ij}(Nj-Ni)}$ can be effectively used to determine the retardation parameters a_d and N_d as well as the fatigue life N_f for specimens subjected to mixed-mode (I and II) overload.

Chapter 3

MATERIAL AND EXPERIMENTATION

3.1 Introduction

This chapter deals with the experimental details and methodology of the present investigation.

3.2. Material

Aluminium alloy 7075 is a high strength material and possesses high yield strength, good fatigue strength and average machinability. It mainly finds its application in aerospace industries especially the structural components expected to experience high stress during service. The alloy is supplied in the form of a 13mm thick plate in T 651 temper condition. The temper condition T651 refers to a treatment consisting of solution heat treatment of material followed by relieving internal stress by stretching, rolling and then artificially ageing it. The chemical composition and mechanical properties of the ally are presented in Tables 3.1 and 3.2 respectively.

Table 3.1 Chemical composition of the AA 7075 T651

Al	Zn	Mg	Cu	Cr	Fe	Si	Ti	Mn	Others
89.6%	6%	2.4%	1.4%	0.18%	0.16%	0.04%	0.05%	0.02%	0.15%

Table 3.2. Mechanical properties of material

Tensile Strength (MPa)	Yield strength (MPa)	Elongation (%)	Hardness (VHN)	Fracture toughness (K_{IC}) (MPa$\sqrt{m}$)
598	557	13	170	26

3.3. Metallography

3.3.1. Metallographic Specimen Preparation

The metallographic examination was done on a small pieces of approximately 12mm x 12mm x 10mm of the as-received material. To examine the microstructure of as-received material, metallographic specimens of the alloy were prepared in three directions: *L-T, L-S,* and *T-S*. The diamond polished specimens were etched with freshly prepared Keller's reagent and examined under optical microscope (Carl Zeiss Microscopy).

3.3.2 Metallographic Examination

The microstructures of all three directions were superimposed to obtain the 3-D view and illustrated in Fig.3.1. The deformed, fibrous and non-recrystallized elongated grain structure may be seen in the micrographs of as-received material.

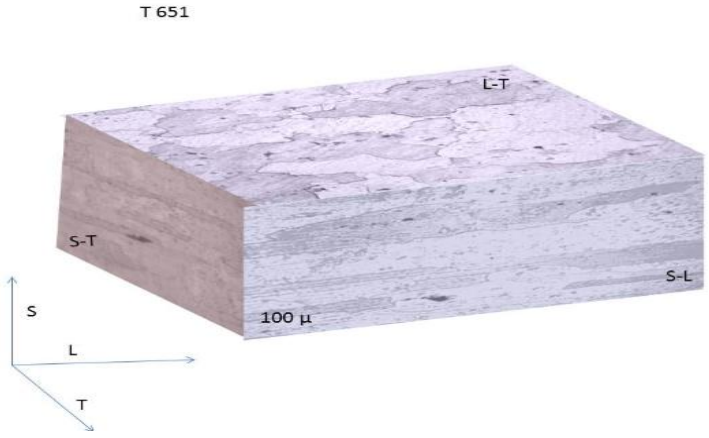

Fig. 3.1- Tri planar optical micrograph of as-received material, etched by Keller's reagent

3.4 Fatigue Crack Growth Test

3.4.1 Test Specimen geometry

Fatigue crack growth tests, were conducted on CT (Compact Tension) specimens with a narrow notch and reduced thickness, fabricated from supplied 13 mm thick plate following ASTM E647-13 [35]. The CT specimens were made in the L-T orientation, loading in longitudinal direction and notch and crack extension in the transverse direction. Both sides of the specimen surfaces were mirror-polish to facilitate visual monitoring of the crack. The

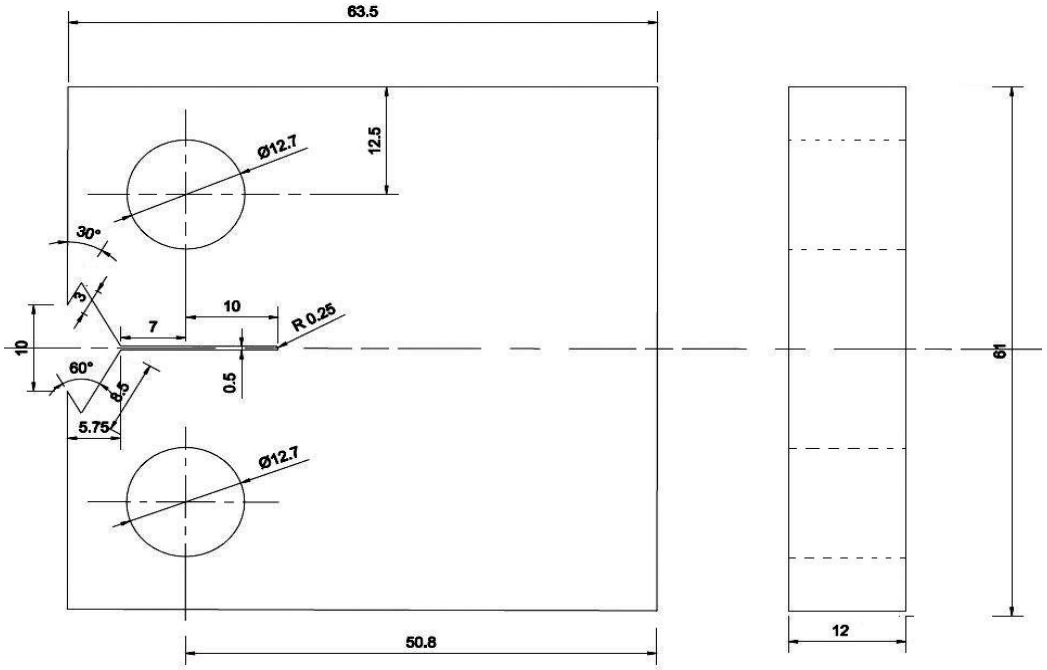

dimensional details of specimen are presented in Fig. 3.2.

.**Fig.**3.2-Compact Tension (CT) Specimen geometry following ASTM E 647-13 [35]

3.4.2 Test equipment Fatigue tests were conducted on 100 kN load capacity *BiSS* servo-hydraulic universal testing machine. The overall arrangement and close-up of the specimen loading may be seen in Fig. 3.3.

Fig. 3.3- Overall arrangements to conduct fatigue crack growth test

Fig. 3.4- Close-up view of the specimen and loading arrangement, COD gauge mounted on the knife edge of the specimen

3.4.3 Test program

Variable amplitude crack propagation (*VAFCP*) software, supplied by the manufacturer of the machine was used to monitor the crack during test with the help of COD gauge, mounted on the knife edges of specimen. The software permitted on-line monitoring of the loads (P and ΔP), crack length (a), compliance, stress intensity factors *(*ΔK, K_{max} *etc)*, crack growth rate (da/dN) etc. All tests were conducted at room temperature maintaining load P=3.97 kN, stress ratio R= 0.3 and test frequency=10Hz and.

3.4.4 Fatigue crack growth tests

The loading of specimen was done as illustrated in Fig. 3.3. Crack opening displacement gauge was mounted on the knife edges of specimen to monitor crack extension. The visual monitoring of crack was also done at regular intervals with the help a low magnification microscope. Fatigue pre-cracking mechanical notched specimen (a/w= 0.24) was done under mode-I loading (crack opening mode) applied load range ΔP= 2.06 kN. Fatigue tests were conducted under following three conditions:

(i) Constant amplitude loading with constant stress ratio (R).

(ii) Constant amplitude loading and single overload cycle introduced at a=14.4mm.

(iii)Constant amplitude loading and band consisting multiple overload cycles at a=14.4mm.

All the tests were conducted in constant load control condition (i.e. increasing ΔK with crack extension), and maintain following loading conditions,

Original a_o/w= 0.187

P_{max}= 3.97kN,

P_{min} = 1.91 kN,

ΔP= 2.06 kN

R= 0.3

Following expressions are used to determine stress intensity factor ranges for CT specimen [38]

$$K = \frac{P}{B\sqrt{w}} * \mathrm{f}\left(\frac{a}{w}\right)$$

Where $f(a/w)=[(2+a/w)(1-a/w)]^{3/2}*[0.886+4.64(a/w)-13.32(a/w)^2+14.72(a/w)^3-5.6(a/w)^4]$

polynomial valid for $\frac{a}{W} \geq 0.2$,

K_{max}= 5.31 MPa√m , ΔK= 3.721 MPa√m at original a_o/w= 0.187

(i) Constant amplitude test:

K_{max}= 5.31 MPa√m , ΔK= 3.721 MPa√m at original $a_o w$= 0.187

K_{max}=12.52 MPa√m , ΔK=4.822 MPa√m at a/w= 0.246

(ii) Constant amplitude loading subjected to an overload spike:

Overload application at a/w= 0.28,

SIF corresponding to maximum of CAL, = K_{max} = 6.96 Mpa√m

Overloading ratio $R_{ol} = \frac{K_{ol}}{K^B_{max}}$= 2.1

Corresponding SIF K_{ol}= 14.616 Mpa√m

(iii)Constant amplitude loading subjected to band consisting multiple overload cycles:

Overload application at a/w= 0.28,

SIF corresponding to maximum of CAL, = K_{max} = 6.96 Mpa√m

Overloading ratio $R_{ol} = \frac{K_{ol}}{K^B_{max}}$= 2.1

Corresponding SIF K_{ol} = 14.616 MPa√m

Number of overload cycles in the bands n = 3, 5, 7, 10, 15 and 20

Frequency of band overloading f_{ol}= 1 Hz

Constant amplitude loading with band (multiple) tensile overload were applied in mode-I, to investigate the effect of a band overload in mode-I. After band overload on the subsequent constant amplitude fatigue crack growth test were allowed for continue the test. The crack was allowed to grow up to $\frac{a}{W} = 0.67$. Band-overload tests were followed by multiple tensile overloads at $\frac{a}{W} = 0.28$, and overload ratio (R_{ol}) was 2.1 and 0.25 Hz frequency. The number of band overload were applied during test are 1, 3, 5, 7, 10, 15 and 20 in the same crack opening mode.

The experimental parameters for all the tests are mentioned in Tables 3.3 and 3.4 respectively.

Tables 3.3 Loading variables for constant amplitude loading condition

P_{max} (kN)	P_{min} (kN)	R	a_o (mm)	f (Hz)
3.97	1.191	0.3	9.5	10

Table 3.4 Loading variables for single overloading and band overloading conditions

P_{max} (kN)	P_{min} (kN)	P_{max}^{ol} (kN)	R	R_{ol}	$(\frac{a}{W})_{ol}$	a_o (mm)	a_{ol} (mm)	f_{ol} (Hz)	f (Hz)
3.97	1.191	8.337	0.3	0.142	0.28	9.5	14.4	1	10

Chapter4

EXPERIMENTAL RESULTS AND DISCUSSIONS

4.1 Introduction`

This chapter deals with experimentally generated crack growth data and their analysis. Fracture surfaces of a few representative specimens were examined under scanning electron microscope and presented at end of this chapter.

4.2 Constant amplitude loading interposed with mode-I overload and band overload

The effect of application of single overload cycle on crack growth behavior is presented in Fig. 1 in the form of crack length vs. number of stress cycle. The application of overload spike has resulted crack growth retardation. The effect of introduction of band overloads during constant amplitude cyclic loading is illustrated in Figs. 3 and 4 in the form of crack length vs. number of stress cycle and FCGR vs. ΔK respectively.

An increase in the magnitude of retardation and drop in the crack growth rate following band overload is observed. The maximum crack growth retardation and maximum drop in the crack growth rate took place on application of band consisting 7-overload cycles. The effects of single overload cycle and band overloads consisting 3 to 20 cycles in terms of delayed cycles, N_d are illustrated in Fig. 4.4 (delayed cycles, N_d is defined in Ch. 2)

The delayed cycle, N_d and minimum crack length corresponding to introduction of 7-overload cycles are $3.75X10^5$ cycles and~$1.5X10^{-6}$ mm/cycle respectively.

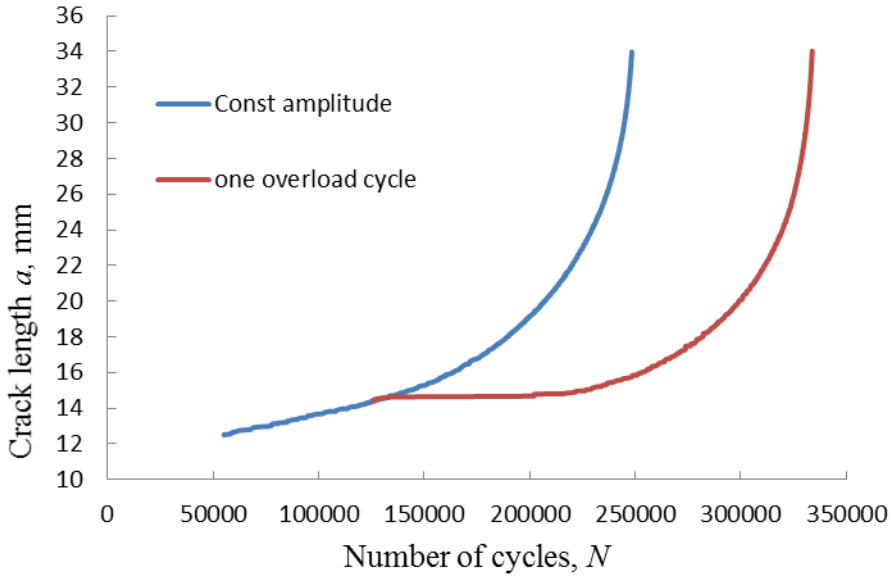

Fig. 4.1- *a-N* plot for Constant amplitude loading and one cycle overload.

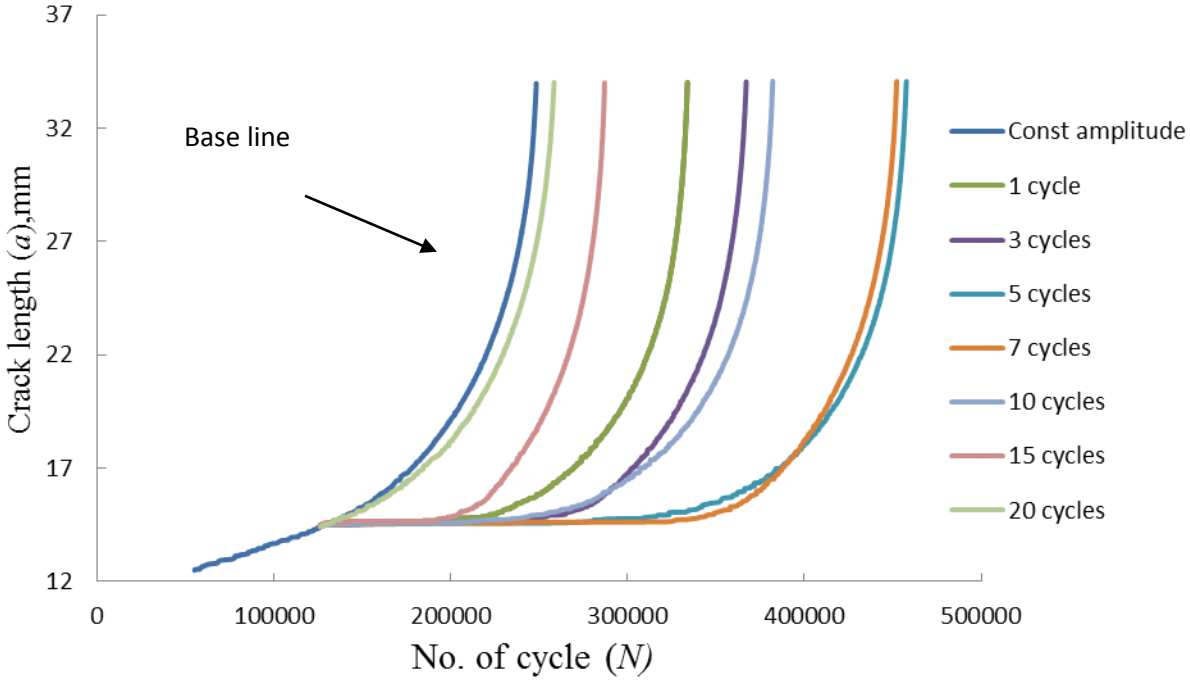

Fig. 4.2- *a-N* plots for different number of overload cycles

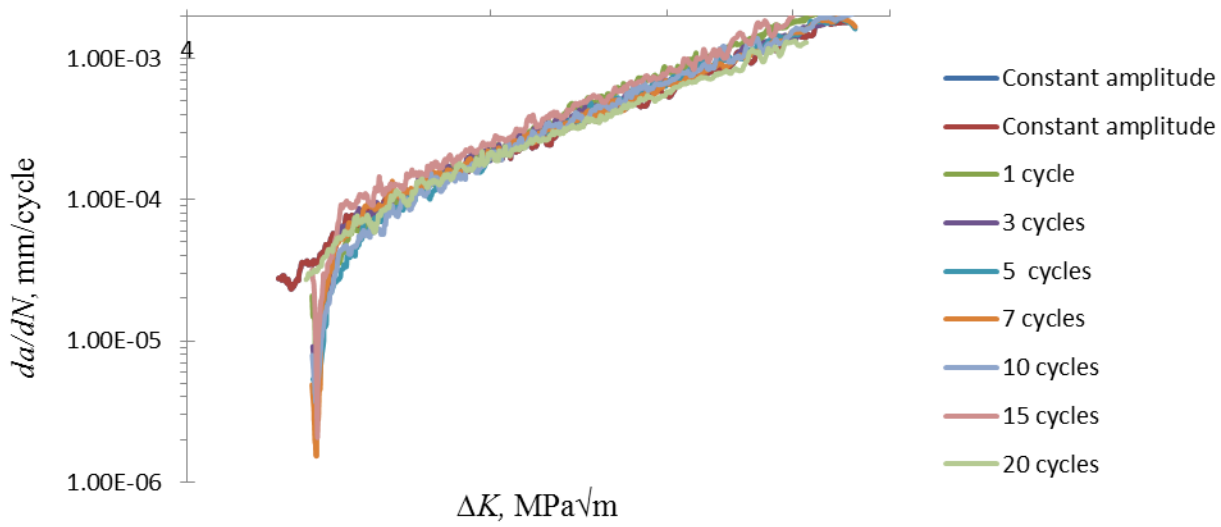

Fig. 4.3- *da/dN*- ΔK plots for different number of overload cycles

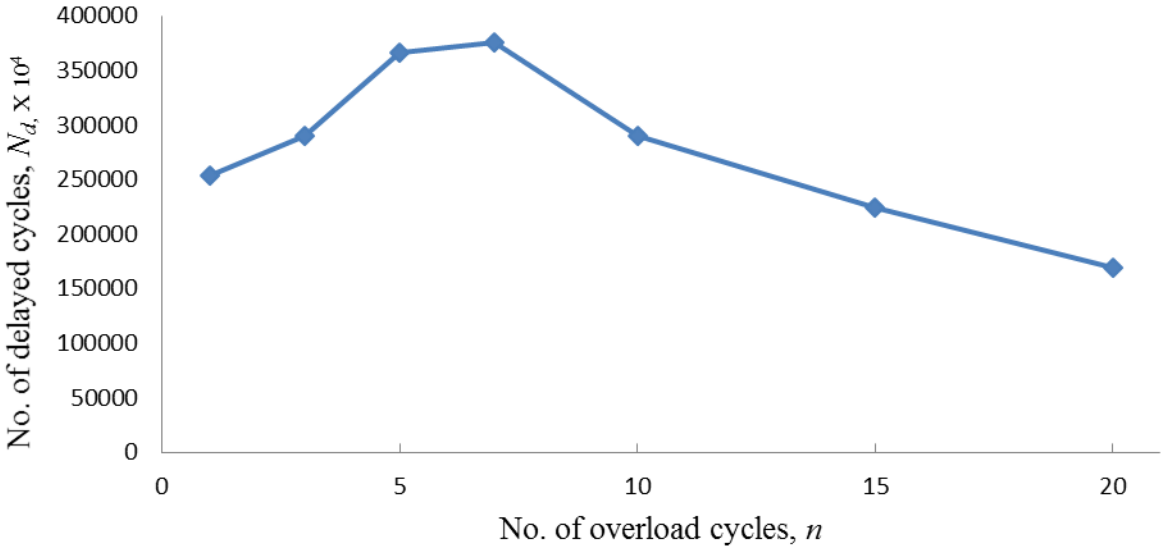

Fig.4.4- Plot of Number of delayed cycles to number of overload cycles

This increase in the magnitude of retardation may be due to development of multiple monotonic plastic zones at the crack tip spread over the extended crack (during band overload application) [36]. The multiple overloading is also expected to strain harden the metal at the crack tip. The strain hardening induced strengthening of metal and application of high magnitude stresses has developed several microvoids and secondary cracks in the stretch zone ahead of the crack tip. The new fracture surfaces associated with microvoids and secondary cracks has reduced the available strain energy required for extension of primary crack, resulting enhanced crack growth retardation. A decrease in crack growth retardation beyond band overload consisting more than 7-overload cycles is also noticed. This may be due to development of large and several secondary cracks their coalescence to develop wide intergranular cracks and subsequently assisted the formation of principal crack [37, 38]. The microvoids, secondary transgranular cracks and secondary intergranular cracks in different overloading condition can be visualized in Figs. 4.5 to 4.9.

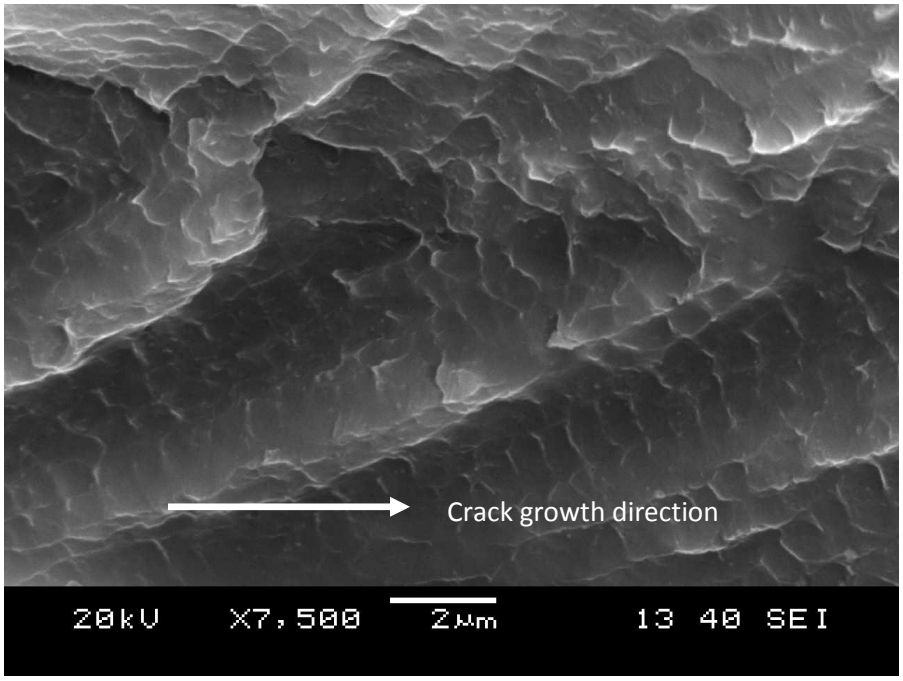

Fig.4.5 - Fractograph of specimen subjected to constant amplitude loading

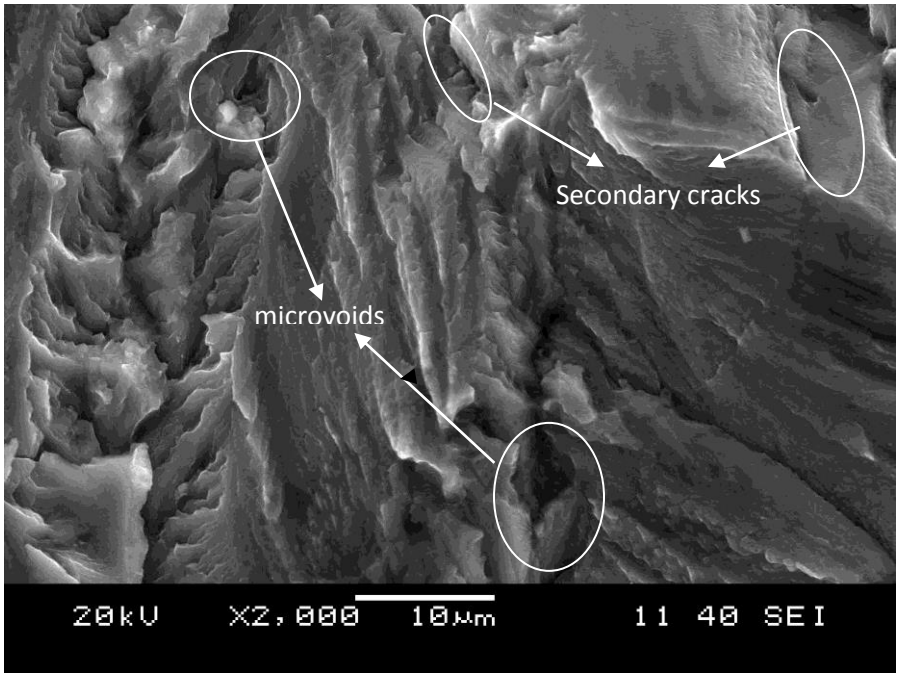

Fig.4.6- Fractograph of specimen subjected to 3 cycle band overloaded specimen

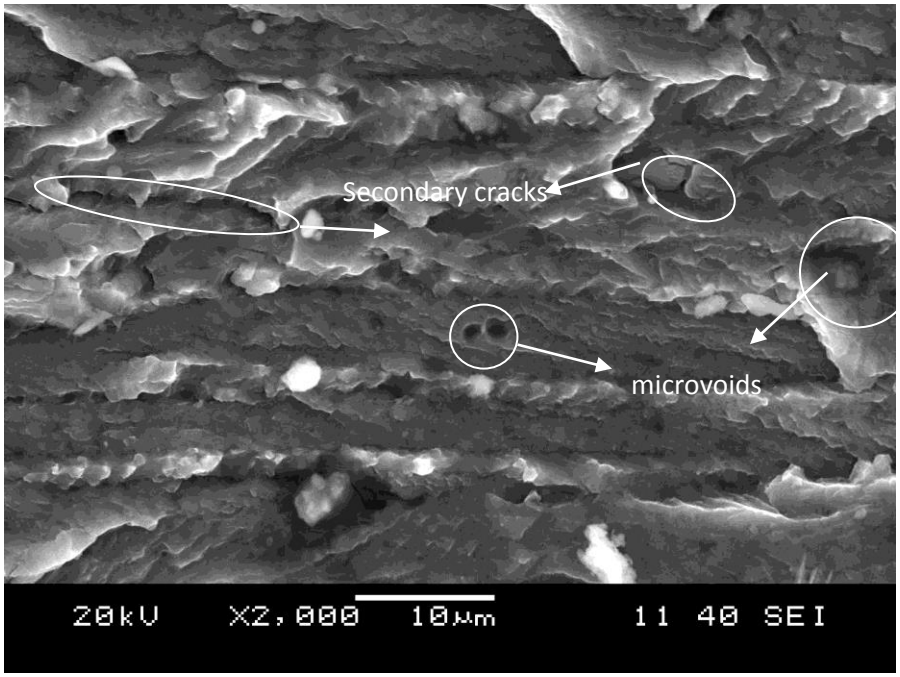

Fig.4.7- Fractograph of specimen subjected to 7 cycle band overloaded specimen

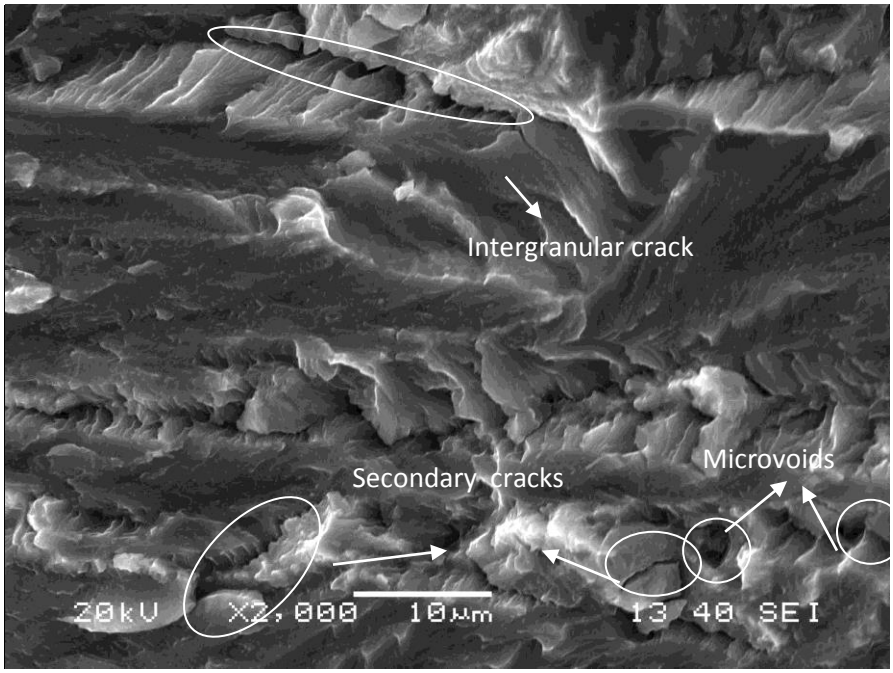

Fig.4.8 -SEM image of fracture surface of 15 cycle band overloaded specimen

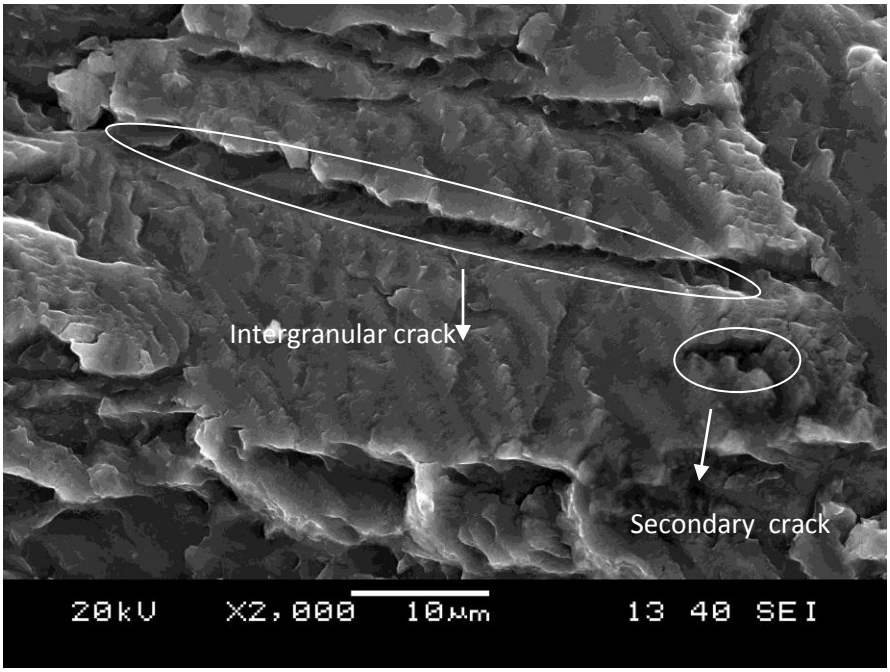

Fig.4.9- Fractograph of specimen subjected to 20 overload cycles

Chapter 5

PREDICTION OF FATIGUE CRACK PROPAGATION USING EXPONETIAL MODEL

5.1 Introduction:

Prediction of fatigue life under variable amplitude loading and band overloading is difficult due to the involvement of various interactive and interrelated variables. Mohanty *et al.* in their work have developed an exponential model for prediction of fatigue crack growth in SENT specimen for constant amplitude loading and variable amplitude loading [34-36]. In the present study an attempt has been made to adopt the exponential model to predict life following stress band consisting several overload cycles. The experimentations have been done on 12.7 mm thick CT aluminium alloy specimens. At the end of this chapter the validation of model has been done with experimental data in order to compare its performance in predicting life.

5.2 Background and approach

Thomas Robert Malthus (1766-1834) first realized that any species can potentially increase according to a geometric series and can follow an exponential law. If a species is having non overlapping populations and each organism produces *R* off spring then population numbers *N* in generation *t*=0, 1, 2 …… is equal to

$$N_1 = N_0.R \text{ And } N_t = N_0.R_t$$

When *t* is large, the above equation can be approximately given by an exponential equation

Population (non-overlapping) of a species after a time interval *t* is expressed as

$$N_t = N_0 . exp(r . t) \qquad (5.1)$$

Where N_0 is the original population of the species, and *r* is Mathusian parameter and also known as intrinsic rate of increase, instantaneous rate of natural increase or specific growth rate.

5.3 Formulation and validation of model

Equation 5.1 can be modified and re-written according to parameters involved in fatigue crack growth as

$$a_j = a_i e^{m_{ij}} \left(N_j - N_i\right) \qquad (5.2)$$

a_i and a_j are crack lengths in i^{th} and j^{th} step respectively. The specific growth rate (m_{ij}), the exponent of the equation is calculated by taking logarithm of the above equation as and expressed as,

$$m_{ij} = \frac{ln\left(\frac{a_j}{a_i}\right)}{(N_j - N_i)} \qquad (5.3)$$

N_i and N_j are number of cycles for i^{th} and j^{th} step respectively

m_{ij}= specific crack growth rate for *i*-*j* interval

i = No. of experimental step and *j*= *i*+1

The specific crack growth rate, *m* is an important term in the model. This can be calculated from crack extension and corresponding number of stress cycles during crack extension. Crack growth in a step can be mainly influenced by applied maximum stress intensity factor in a cycle K_{max}, stress intensity factor range ΔK, stress intensity factor corresponding to the applied overload K_{ol}, number of applied overload cycles and material properties (i.e., fracture toughness K_c, yield strength of the material σ_{ys} and modulus of elasticity E_m).

The specific growth rate can be expressed as a function of dimensionless quantities in terms of above mentioned variables and expressed as,

$$m = f\{\left[\left(\frac{\Delta K}{K_C}\right)\left(\frac{K_{max}}{K_C}\right)\left(\frac{\sigma_{YS}}{E_m}\right)\right]^{1/4} * [\frac{1}{n+1}]\} \qquad (5.4)$$

Equation (5.4) can be simplified as,

$$m = f(l)$$

Where,

$$l = \left[\left(\frac{\Delta K}{K_C}\right)\left(\frac{K_{max}}{K_C}\right)\left(\frac{\sigma_{YS}}{E_m}\right)\right]^{1/4} * \left[\frac{1}{n+1}\right] \qquad (5.5)$$

Following polynomial is used to calculate stress intensity factor range, ΔK ,

$$\Delta K = \frac{\Delta P}{B\sqrt{w}} * f(\frac{a}{w}) \qquad (5.6)$$

Here $f(a/w)=[(2+a/w)(1-a/w)]^{3/2}*[0.886+4.64(a/w)-13.32(a/w)^2+14.72(a/w)^3-5.6(a/w)^4]$

In this model fourth order polynomial equation is used to predict the values of *m* for different values of *l*.

Let $m = Al^4 + Bl^3 + Cl^2 + Dl + E$ (5.7)

A fourth order degree polynomial

Where, $l = \left[\left(\frac{\Delta K}{K_C}\right)\left(\frac{K_{max}}{K_C}\right)\left(\frac{\sigma_{YS}}{E_m}\right)\right]^{1/4} * \left[\frac{1}{n+1}\right]$ and *A, B, C, D, E* are material constants.

The different *m* and *l* values are fitted in fourth order degree polynomial equation of post overload portion for six specimen for different number of overload cycles (*n* =1, 3, 5, 7, 10, 15). The predicted *m* values are calculated from the above equation and values of constants *A, B, C, D,* and *E* for each overload cycle are tabulated in Table 5.1

Table.5.1 Values of constants *A, B, C, D* and *E* for band consisting different number of overload cycles

Number of overload cycles, *n*	*A*	*B*	*C*	*D*	*E*
1	-0.0007	0.0028	-0.0018	0.00004	-2E-05
3	-0.1835	0.0848	-0.0144	0.0011	-2E-05
5	-2.8465	0.7497	-0.0708	0.0029	-2E-05
7	-3.8322	0.8383	-0.0657	0.0023	-2E-05
10	-14.927	2.4165	-0.1425	0.0037	-2E-05
15	-71.71	7.8003	-0.3151	0.0058	-2E-05

5.3.1 Validation of model

Since the above constants are different for different number of overload cycles, therefore they are correlated with number of overload cycles. In order to find material constant at any number of overload cycles, a set of polynomial equations are written and expressed as,

A=-0.049n^3+0.585n^2-2.58n+1.99 (5.8)

B=0.003 n^3-0.038 n^2+0.262n-0.206 (5.9)

C=0.0012 n^2-0.0021n-0.0053 (5.10)

D=-4.32 n^2+0.0004n-0.0001 (5.11)

The number of cycles or fatigue life is predicted using equations 5.4 to 5.7 and finally the following equation,

$$N_J = \frac{ln\left(\frac{a_j}{a_i}\right)}{m_{ij}} + N_i \quad (5.12)$$

The data generated following different overload cycles are subsequently utilized to estimate specific growth rate (m_{ij}) and develop a- N plot corresponding to a stress band consisting 20 overload cycles.

The a-N curve obtained from proposed exponential model and that obtained from experimental data have been compared in Fig. 5.1. The corresponding FCGR vs. ΔK curves is presented in Fig. 5.2. It can be seen in Fig. 5.1 that the predicted crack length is marginally less than the experimental data. On the other hand the model overestimated the crack growth rate, da/dN especially in the higher ΔK region.

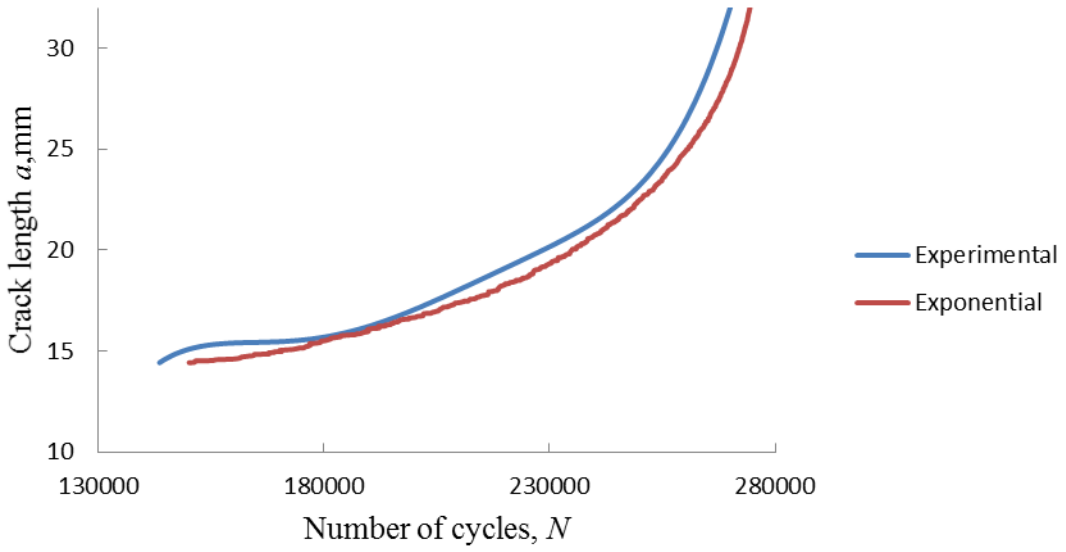

Fig. 5.1- a-N plot of experimental data vs. predicted data for band overload of 20 cycles

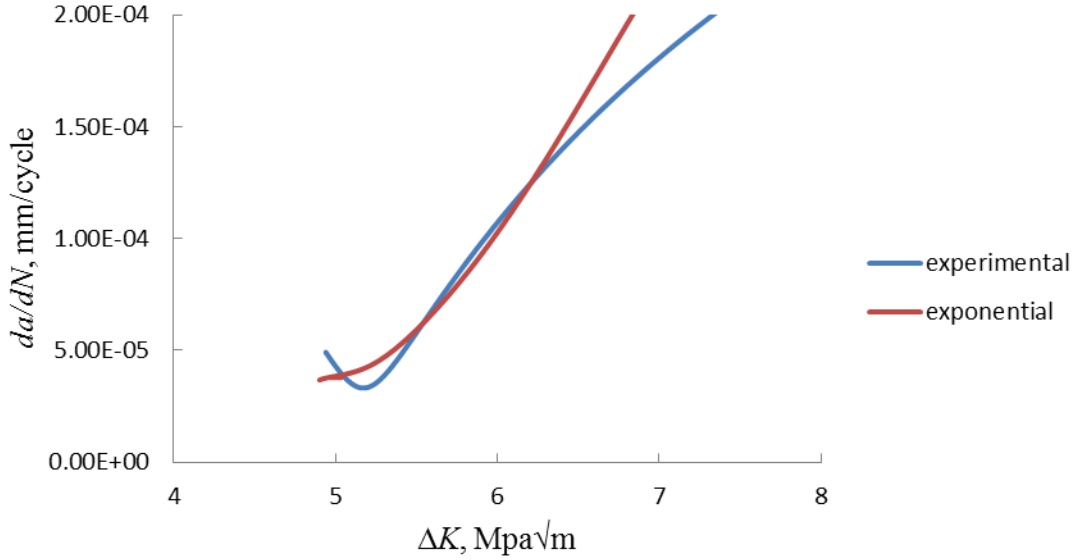

Fig. 5.2- *da/dN vs.* ΔK plots of experimental data vs. predicted data for band overload of 20 cycles.

Chapter 6

PREDICTION OF FATIGUE CRACK PROPAGATION USING GAMMA MODEL

6.1 Introduction

In order to estimate the post overload fatigue crack growth a gamma function is attempted in this chapter. The gamma function can be correlated with various physical variables like crack driving parameters and materials parameters in a non-dimensional to widen its acceptability. At the end of this chapter the validation of model has been done with experimental data in order to compare its effectiveness in predicting life.

6.2 Background and approach

In 18th century the Swiss mathematician Leonhard Euler introduced Gamma function. It is defined as the generalization of the factorial function to non-integral values. The factorial (written as $n!$) for a positive whole number n, is defined by $n! = 1 \times 2 \times 3 \times \ldots \times (n-1) \times n$. This expression is meaningful if n is an integer. In order to extend the factorial to any real number $n > 0$ (whether or not n is a whole number), the gamma function is defined as:

$$\Gamma(z) = \int_0^N t^{z-1} e^{-t} dt, Re(z) > 0 \qquad (6.1)$$

In this chapter a modified gamma model has been proposed to predict crack growth in compact tension specimens. The term *t* is replaced by number of stress cycles *N*. The parameter *z* is non-dimensional and represents the properties that affect crack growth. As, fatigue crack growth depends on the initial crack length, material properties and specimen geometry, loading conditions etc. The integral is chosen in such a way that it is non-dimensional and includes all the above mentioned variable and estimates crack growth at the end of a fixed number of loading cycles. Therefore, the relation for predicting the final crack length at the end of *N* cycle is given by,

$$\frac{ma_1}{w} = \int_0^N N^{\left(\frac{ma_0}{w}-1\right)} e^{-N} dN \tag{6.2}$$

In this equation, *w* is the specimen width, and *m* is defined as a non-dimensional parameter whose value remain approximately constant for a given cycle interval. The value of *m* includes all the properties which affect crack growth and expressed as,

$$m = Al^5 + Bl^4 + Cl^3 + Dl^2 + El + F \tag{6.3}$$

A, *B*, *C*, *D*, *E* and *F* are curve fitting constants. The non-dimensional term *m* is correlated with another parameter *l* which takes into account two crack driving forces, ΔK and K_{max} as well as material properties K_c, *E*, σ_{ys} and is expressed as,

$$l = \left[\left(\frac{\Delta K}{K_C}\right)\left(\frac{K_{max}}{K_C}\right)\left(\frac{\sigma_{YS}}{E}\right)\right]^{1/4} * \left[\frac{1}{n+1}\right] \tag{6.4}$$

6.3 Formulation and validation of model

Based upon the experimental data a program was developed in Java for determining the non-dimensional term *m*. This is calculated for each step in incremental manner along with the crack length by using gamma function.

6.3.1 Formulation of model

The modified gamma function is given as,

$$\frac{ma_1}{w} = \int_0^N N^{\left(\frac{ma_0}{w}-1\right)} e^{-N} dN \qquad (6.5)$$

Where *w* is the specimen width, and *m* is the non-dimensional term whose value remain constant for a given small cycle interval. Initially, value of *m* is assumed for a given interval of cycle. For a given interval of cycle the experimental values of a_0, *w*, a_1, *N* are used for the processing of term *m*. The value of *m* for which LHS and RHS of the Eq.6.5 became nearly equal ($\pm$ 0.01) is used to predict *a* vs. *N* plot.

The RHS of equation (6.5) was solved with the help of Java programming which is described as follows

6.3.2 Validation of model:

The value of *m* is correlated with all the properties which affect crack growth. Therefore value of *m* is given by:

$$m = Al^5 + Bl^4 + Cl^3 + Dl^2 + El + F \qquad (6.6)$$

where *A, B, C,*D, E and F are curve fitting constants whose average value for six specimens (1, 3, 5, 7, 10, 15) have been presented in the Table 6.1. The specific growth rate *m* is correlated with another parameter *l* which takes into account two crack driving forces ΔK and K_{max} as well as material parameters K_c, *E*, σ_{YS} and is represented by equation:

$$l = \left[\left(\frac{\Delta K}{K_C}\right)\left(\frac{K_{max}}{K_C}\right)\left(\frac{\sigma_{ys}}{E_m}\right)\right]^{1/4} * \left[\frac{1}{n+1}\right] \quad (6.7)$$

The stress intensity *K* has been calculated by equation [8],

$$\Delta K = \frac{\Delta P}{B\sqrt{w}} * f\left(\frac{a}{w}\right) \quad (6.8)$$

Where $f(a/w)=[(2+a/w)(1-a/w)]^{3/2}*[0.886+4.64(a/w)-13.32(a/w)^2+14.72(a/w)^3-5.6(a/w)^4]$

The crack length is calculated as:

$$a_1 = \frac{w}{m} * \int_0^N N^{\left(\frac{ma_0}{w}-1\right)} e^{-N} dN \quad (6.9)$$

Here *m* has been given by Eq.6.6 after substituting value of curve fitting constants (for six specimens) and validate it by using Eq. 6.9 for specimen subjected to band consisting 20 overload cycles.

The experimental *a-N* data of specimens subjected to overload cycles 1, 3, 5, 7, 10, 15 are used for formulation of model, and its validation has been checked on specimen imposed 20 overload cycles. The predicted *a-N* curve obtained from proposed gamma model is compared with experimental test data in Fig. 6.1. The different *m* and *l* values are fitted by 5^{th} degree polynomial equation of post overload portion. The predicted *m* values are calculated as per the Eq. 6.6 from the values of constants *A, B, C, D,* E and F tabulated in Table.6.1 for each number

of overloading conditions. Eqs. 6.6- 6.9 are subsequently used to predict crack length corresponding to given number of stress cycles for specimen subjected to 20-overload cycles. The predicted and experimental *a*-*N* and d*a*/d*N*- Δ*K* plots are presented in Figs. 6.1 and 6.2 respectively. The model is capable of predicting crack growth behaviour satisfactorily. However, the model underestimates FCGR over entire range of applied Δ*K*.

Table.6.1 Values of constants *A, B, C, D,* E and F for band consisting different number of overload cycles

Number of overload cycles, *n*	*A*	*B*	*C*	*D*	*E*	*F*
1	-48078	4758	-1832.5	347.21	-33.67	0.9991
3	-192254	91577	-16986	1551.5	-72.57	0.9992
5	-1E+06	396837	-51191	3236.5	-104.13	1.9245
7	-2E+07	3E+06	-255648	9313.4	-171.82	0.9999
10	-2E+07	4E+06	-270389	9708.4	-176.76	0.9999
15	-1E+08	2E+07	-904304	21688	-246.07	0.9991

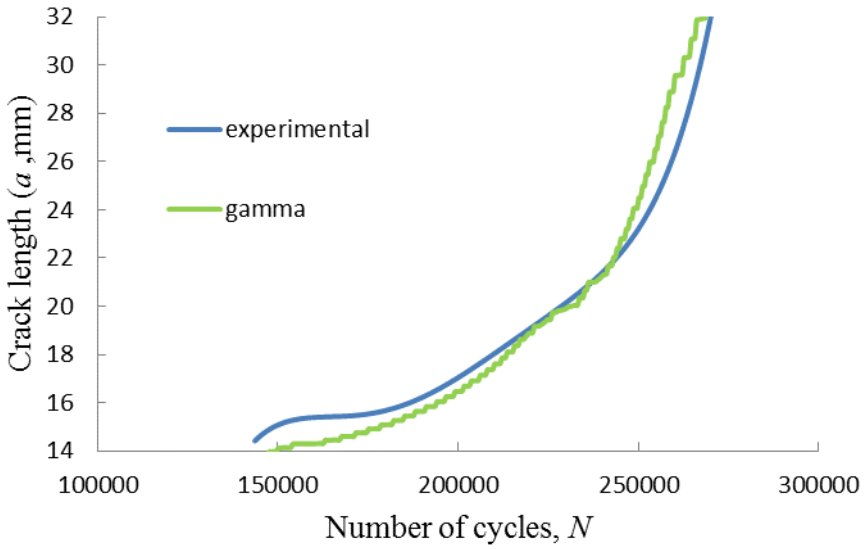

Fig. 6.1 *a-N* plot of experimental data vs. predicted data for band overload of 20 cycles

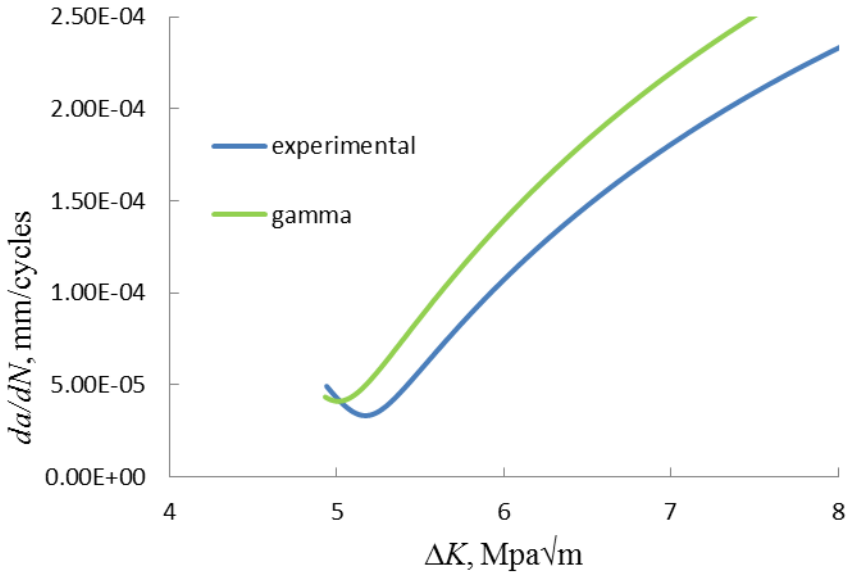

Fig. 6.2 d*a*/d*N vs.* Δ*K* plots of experimental data vs. predicted data for band overload of 20 cycles

Chapter 7

COMPARISION OF RESULTS AND DISCUSSIONS

7.1 Introduction

The magnitude of retardation is usually expressed as delayed cycle, N_d and retarded crack length a_d. This Chapter is devoted to study the performance characteristics of proposed exponential and gamma model in terms of these two retardation parameters. Finally, a brief discussion has been provided describing the relative merits and limitations of the proposed models.

7.2 Comparison of predicted and experimental results

The performance of exponential model and gamma model are evaluated by comparing the predicted results with experimental data in terms of N_d and a_d. There are two criteria that have been used for comparison of predicted results and experimental data, which are,

1. Percent deviation is defined as difference of predicted value and experimental value with respect to experimental value,

$$\%\ Deviation = \frac{Predictedvalue - Experimental\ value}{Experimentalvalue} * 100$$

2. Prediction ratio which is defined as ratio between experimental data to predicted result as,

$$Prediction\ ratio P_r = \frac{Experimental\ value}{Predictedvalue}$$

The *a*-*N* plots based on experimental data, gamma and exponential models based data for specimen subjected to 20 cycles band overload is presented in Fig. 7.1. The experimental and predicted d*a*/d*N* vs *a*. plots are illustrated in Fig. 7.2. The values of retarded crack length a_d are obtained from this figure and tabulated in Tables 7.1 and 7.2. The FCGR vs. Number of stress cycle plots of are presented in Fig. 7.3.

Retardation parameter, delayed number of stress cycle N_d is obtained for each plot and tabulated in Tables 7.1 and 7.2 from this plot. The prediction ratio, P_r >1 signifies under predicted result while P_r <1 signifies over predicted result.

Table.7.1 Comparison of Exponential model data with Experimental data in terms of delayed crack length a_d and delayed number of cycles N_d for 20 cycles band overload

a_d Exponential, mm	a_d Experimental, mm	% Error	N_d Exponential, cycles	N_d Experimental, cycles	% Error
15.61	16.22	-3.822	195100	189100	3.17

Table 7.2 Comparison of Gamma model data with Experimental data in terms of delayed crack length a_d and delayed number of cycles N_d for 20 cycles band overload

a_d Gamma, mm	a_d Experimental, mm	% Error	N_d Gamma, cycles	N_d Experimental, cycles	% Error
15.36	16.22	-5.30	184100	189100	-2.64

From Table 7.3, it is seen that both models under predicts retarded crack length, a_d (P_r >1), which is good.

From Table 7.4, it is seen that exponential model over predicts delayed number of cycles, N_d (P_r <1) while gamma model under predicts (P_r >1). Under prediction of delayed number of cycles is always better and hence, in this regard, gamma model scores marginally better.

Table 7.3 Model Performances (for crack length) by percentage deviation of retardation parameter a_d.

Test specimen	% Deviation (exponential model) (a_d)	% Deviation (gamma model)	Prediction ratio (exponential model)	Prediction ratio (gamma model)
CT specimen(20 overload cycles)	-3.822	-5.30	1.03	1.05

Table 7.4 Model Performances (for number of cycles) by percentage deviation of retardation parameter N_d

Test specimen	% Deviation (exponential model) (N_d)	% Deviation (gamma model)	Prediction ratio (exponential model)	Prediction ratio (gamma model)
CT specimen(20 overload cycles)	3.17	-2.64	0.96	1.02

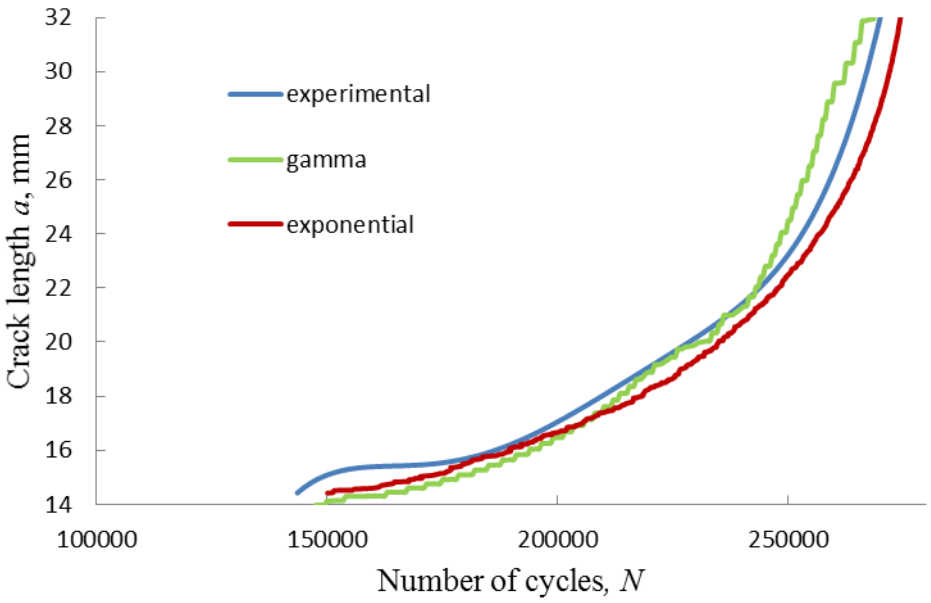

Fig.7.1 *a*-*N* plot for experimental and predicted exponential model and gamma model (20 cycles)

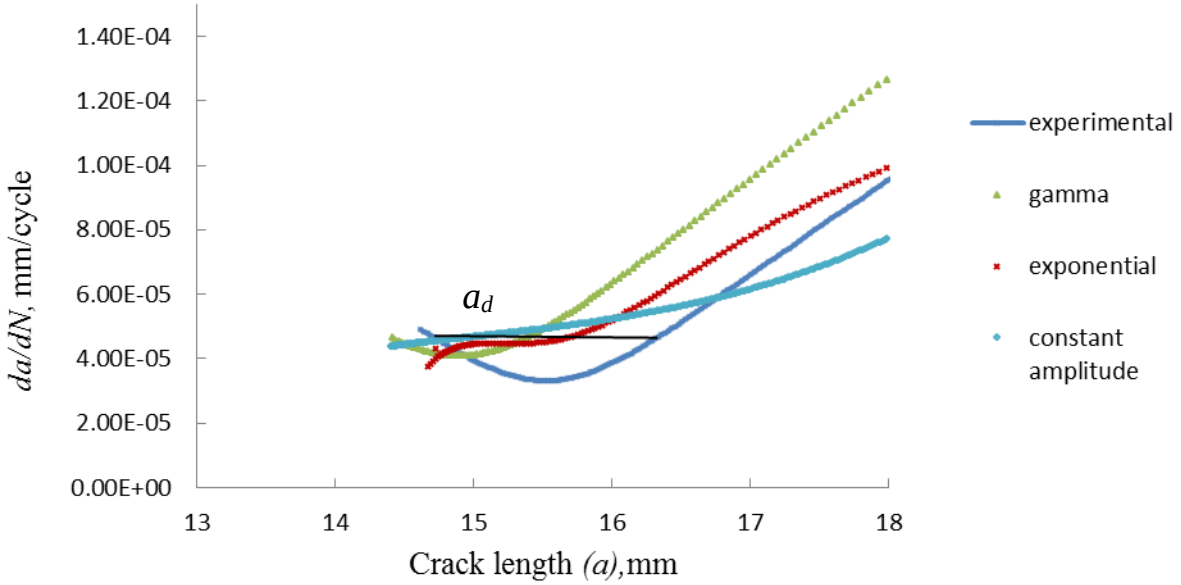

Fig.7.2-*da/dN* vs. *a* plot of constant amplitude and experimental and predicted values for 20 cycles overload band.

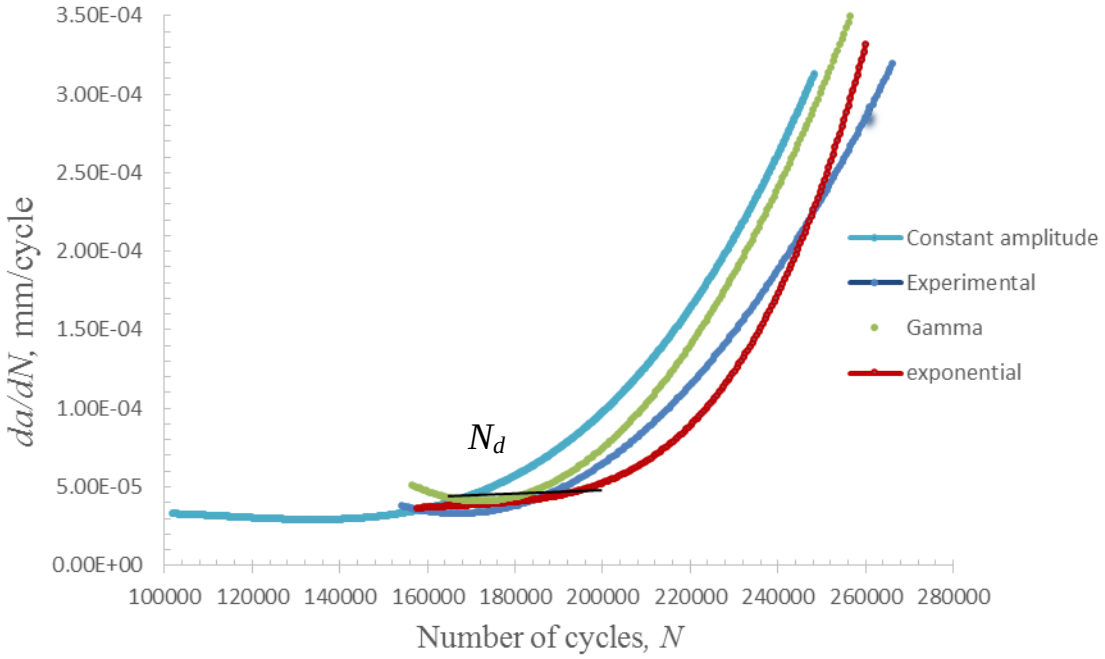

Fig.7.3 *da/dN* vs. *N* plot of constant amplitude and experimental and predicted data for 20 cycles overload band.

Chapter 8

CONCLUSION AND FUTURE WORK

CONCLUSIONS

1. It is observed that there is crack growth retardation following single overload as well as band overload. The maximum retardation occurs for band over load consisting 7 overload cycles under present loading conditions and specimen geometry.
2. Exponential model of the form $a_i = a_j e^{m_{ij}(N_j - N_i)}$ can be used to determine the fatigue crack propagation for post band overload without going through numerical integration.
3. Gamma model of the form $\frac{ma_1}{w} = \int_0^N N^{\left(\frac{ma_0}{w}-1\right)} e^{-N} dN$ has been developed and effectively used to determine the fatigue crack propagation in CT specimen.
4. Using the above models it is possible to predict the crack extension corresponding to a given number of cycles or to predict the number of cycles required for a given crack extension. Both the models are capable of predicting crack growth behaviour satisfactorily. However, percent deviation for Gamma model is marginally more than that for exponential model.
5. From the analysis of predicted results it is seen that both models under predict delayed crack length (Pr >1), which is good.

The exponential model over predicts delayed number of cycles (Pr <1) while gamma model under predicts (Pr >1). Under prediction of delayed number of cycles is always better and hence, in this regard, gamma model scores marginally better.

SUGGESTED FUTURE WORK

1. The proposed exponential model and gamma model may be attempted to predict fatigue crack propagation under variable amplitude loading condition at different temperatures.
2. The proposed models may be attempted for other specimen geometries.

REFERENCES

[1] Suresh S, Vasudevan AK, Bretz PE. "Mechanism of slow fatigue crack growth in high strength aluminum alloys", Metal Trans, 15A, pp.369, 1984

[2] Brog TK, Jones JW, Was GS," Fatigue Crack Growth Retardation of INCONEL600." Engineering Fracture Mechanics, 20 No. 2, pp. 313-320, 1984

[3] Kumar R, Singh SB, "Investigation of fatigue crack growth after a single cycle peak overload in IS 1020 steel," Int J Press Vess Pip, 51, pp. 25–35, 1984

[4] Gan D, Weertman J," Fatigue crack closure after overload," Eng Fract Mech, 18(1), pp.155–60, 1983

[5] Sander M, Richard HA," Finite element analysis of fatigue crack growth with interspersed mode-I and mixed mode overloads", International Journal of Fatigue, 27 ,pp. 905-913, 2005

[6] Sander M, Richard HA. "Experimental and numerical investigations on the influence of the loading direction on the fatigue crack growth". Int. J. of. Fatigue. 28, pp. 583-591, 2006

[7] Forman RG, Kearney VE, Engle RM, "Numerical analysis of crack propagation in cyclic-loaded structures," J of Basic Engg., 89, pp. 459-464,1967.

[8] Walker K, "The effect of stress ratio during crack propagation and fatigue for 2024-T3 and 7075-T6 aluminium," In Effects of Environment and Complex Load History for Fatigue Life, ASTM STP, l. 462, pp. 1-14, 1970.

[9] Wheeler OE, "Spectrum loading and crack growth," J. of Basic Engg.,. 94,pp. 181-186, 1972.

[10] Willenborg JD, Engle RM, and Wood HA, "A crack growth retardation model using an effective stress concept," Report AFFEL-TM-71-1- FBR, Dayton (OH), Air Force Flight Dynamics Laboratory, Wright–Patterson Air Force Base, 1971.

[11] Corbley DM, Packman PF, "On the influence of single and multiple peak on fatigue crack propagation in 7075-T6511 aluminium," Engg. Fract. Mech. 5, pp. 479-497, 1973.

[12] Taheri F, Trask D, and Pegg N, "Experimental and analytical investigation of fatigue characteristics of 350WT steel under constant and variable amplitude loadings," J.of Marine Struct., 16, pp. 69-91, 2003.

[13] Chang JB, Hudson CM., "Methods and models for predicting fatigue crack growth under random loading," ASTM STP, 748, 1981.

[14] Bannantine Julie A, Comer Jess J, Handrock James L, "Fundamentals of Metal Fatigue Analysis, Prentice Hall", Englewood Cliffs, New Jersy 1990.

[15] Ellyin F, Li HP. "Fatigue crack growth in large specimens with various stress ratios". Journal of Pressure Vessel Technology. 106, pp. 255–260, 1984.

[16] Bannantine Julie A, Comer Jess J, Handrock James L. Fundamentals of Metal Fatigue Analysis, Prentice Hall, Englewood Cliffs, New Jersy 1990.

[17] Benachour M , Benachour N, Benguediab M." Effect of Single Overload Ratio and Stress Ratio on Fatigue Crack Growth", 7), pp. 1, 2013.

[18] Gdoutos EE. Fracture Mechanics- An Introduction, Springer, 2005.

[19] Broek D, Elementary Engineering Fracture mechanics, Martinus Nijhoff Publishers, The Hague, 1982.

[20] Anderson TL, Fracture Mechanics: Fundamentals and Applications. Boston CRC Press, 1995.

[21] Verma BB, Pandey RK. Effect of loading variables on overload induced delay cycle in fatigue. In: Proceedings of the Third Workshop on Creep, Fatigue and Creep–Fatigue Interaction. Kalpakkam, India: Indira Ghandi Centre for Atomic Research, 1998:C1–8.

[22]. Raghuvir Kumar, Garg SBL, “Effect of Periodic Bands of Overloads on Crack Closure “, Int. J. Pres. Ves. & Piping 38, pp.27-3, 1989.

[23]. Luiz Fernando Martha, Evaluation of crack growth retardation in branched fatigue cracks Marco Antonio Meggiolaro 1 Antonio Carlos de Oliveira Miranda,Jaime Tupiassú Pinho de Castr,

[24] McMillan JC, Pelloux RMN. "Fatigue Crack Propagation under Program and Random Loads," ASTM STP 415, American Society for Testing and Materials, Philadelphia, 1967.

[25] Jones RE, “Fatigue Crack Growth Retardation After Single-Cycle Peak Overload in Ti6A1-4V Titanium Alloy”, Engineering Fracture Mechanics 5, 1973.

[26] Wei RP, Shih TT, “Delay in Fatigue Crack Growth”, Int. J. of Fracture, 10, 1974.

[27] Wheeler OE, Spectrum Loading and Crack Growth. General Dynamics Report FZM-5602, Fort Worth, 1970.

[28] Elber W, “The Significance of Crack Closure, Damage Tolerance in Aircraft Structures. ASTM STP 486, American Society for Testing and Materials, Philadelphia, pp. 230-242. 1971.

[29] Paris PC, and Erdogan F, “A critical analysis of crack propagation laws,” J. of Basic Engg., vol. 85, pp. 528-534, 1963.

[30] Spagnoli A, “Self-similarity and fractals in the Paris range of fatigue crack growth,” Mech. Mat., vol. 37, pp. 519-529, 2005.

[31] Maymon G, “The problematic nature of the application of stochastic crack growth models in engineering design,” Engg. Fract. Mech., vol. 53, No. 6, pp. 911-916, 1996.

[32] Mohanty JR., Verma BB, Ray PK., "Prediction of fatigue crack growth and residual life using an exponential model: Part II (mode-I overload induced retardation)." Int. J. of Fatigue, vol. 31(III), pp. 425-432, 2009.

[33] Mohanty JR, Verma BB, Ray PK., "Evaluation of overload-induced fatigue crack growth retardation parameters using an exponential model." Engineering Fracture Mechanics, vol. 75(XIII), pp. 3941-3951, 2008.

[34] Mohanty JR., Verma BB, and Ray PK., "Prediction of fatigue life with interspersed mode-I and mixed-mode (I and II) overloads by an exponential model: extensions and improvements." Engineering Fracture Mechanics, vol. 76(III), pp. 454-468, 2009.

[35] Standard Test Method for Measurement of Fatigue Crack Growth Rates, Annual Book of ASTM Standards, E647, 2013.

[36] Abhinay SV *et al*.," Effect of band overload on fatigue crack growth rate of HSLA steel," IOP Conf. Ser.: Mater. Sci. Eng. 75 012010, 2015.

[37] Lehr KR. and Liu HW, International journal of fracture mechanics, vol.5,, p45, 1969

[38] Sahu VK, Anil Kumar JKS, Verma BB, Ray PK "Effect of low temperature overload on fatigue crack growth retardation and prediction of post overload fatigue life, Aerospace and technology 33, pp.100-106, 2015.

ANNEXURE

Java Programming

```
import java.io.BufferedReader;
import java.io.BufferedWriter;
import java.io.FileNotFoundException;
import java.io.FileReader;
import java.io.FileWriter;
import java.io.IOException;

public class NumericalIntegration
{

        interface FPFunction
        {
          double eval(double n);
        }

        public static double simpsons(double a, double b, int n, FPFunction f)
        {
          double range = checkParamsGetRange(a, b, n);
          double nFloat = (double)n;
          double sum1 = f.eval(a + range / (nFloat * 2.0));
```

```
  double sum2 = 0.0;
  for (int i = 1; i < n; i++)
  {
    double x1 = a + range * ((double)i + 0.5) / nFloat;
    sum1 += f.eval(x1);
    double x2 = a + range * (double)i / nFloat;
    sum2 += f.eval(x2);
  }
  return (f.eval(a) + f.eval(b) + sum1 * 4.0 + sum2 * 2.0) * range / (nFloat * 6.0);
}

private static double checkParamsGetRange(double a, double b, int n)
{
  if (n <= 0)
    throw new IllegalArgumentException("Invalid value of n");
  double range = b - a;
  if (range <= 0)
    throw new IllegalArgumentException("Invalid range");
  return range;
}
```

```
private static double testFunction(String fname, double a, double b, int n, FPFunction
f)
{
  return simpsons(a, b, n, f);
}

public static void main(String[] args) throws FileNotFoundException
{
    System.out.println("Started");

  //Delimiter used in CSV file
  String COMMA_DELIMITER = ",";
  String NEW_LINE_SEPARATOR = "\n";
  String FILE_HEADER = "a0,a1,m";

  BufferedReader fileReader = null;
  FileWriter fileWriter = null;
  try{
      int count = 0;
      String line = "";

      //Reading from csv files
```

```
                    fileReader = new BufferedReader(new
FileReader("C:/Users/Naresh/Desktop/Abhinay/15cycles_input.csv"));
                    fileWriter = new
FileWriter("C:/Users/Naresh/Desktop/Abhinay/15cycles_output.csv");
                    BufferedWriter out = new BufferedWriter(fileWriter);

                    //Read the CSV file header to skip it
                    fileReader.readLine();
                   //Write the CSV file header
                   out.write(FILE_HEADER.toString());
                   out.write(NEW_LINE_SEPARATOR);

                   double i = 1.0;
                    while ((line = fileReader.readLine()) != null) {
                  //Get all tokens available in line
                  String[] tokens = line.split(COMMA_DELIMITER);
                  tokens[0] =  tokens[0].substring(1);
                  tokens[1] = tokens[1].substring(0, tokens[1].length() - 1);

                  if (tokens.length > 0) {
                     //Logic to find the m value
                     Double Da0 = Double.valueOf(tokens[0]) ;
                        double w = 50.7;
```

```
                    Double Da1 = Double.valueOf(tokens[1]);
                    double finalvalue = 1000;
                    double a0 = Da0.doubleValue();
                    double a1 = Da1.doubleValue();

                    for(double m = i ; m <= 1.0 ; m = m - 0.01)
                    {
                        final double x = ((m*a0)/w) - 1;
                          double rhs = testFunction("2.7183^x", 1, 500, 499000, new
FPFunction() {
                              public double eval(double n) {
                                return  Math.pow(n,x) * Math.exp(-n);
                              }
                            }
                          );

                          double lhs = (m*a1)/w;

                          if(lhs-rhs < 0.01){
                                finalvalue = m;
                                i = m+0.03;
                                break;
                          }
```

```
                }


                out.write(String.valueOf(a0));
                out.write(COMMA_DELIMITER);
                out.write(String.valueOf(a1));
                out.write(COMMA_DELIMITER);
                out.write(String.valueOf(finalvalue));
                out.write(NEW_LINE_SEPARATOR);
            }
        }
                out.flush();
                out.close();
     }catch (Exception e) {
    System.out.println("Error in CsvFileReader !!!");
    e.printStackTrace();
} finally {
    try {
        fileReader.close();
    } catch (IOException e) {
        System.out.println("Error while closing fileReader !!!");
        e.printStackTrace();
```

```
            try {
                fileWriter.flush();


                    fileWriter.close();
                } catch (IOException oe) {
                    System.out.println("Error while flushing/closing fileWriter !!!");
                    oe.printStackTrace();


                }
            }
        }
            System.out.println("Flushed");
    return;
  }
}
```

List of Publications and Conferences

1. Effect of band-overload on fatigue crack growth rate of HSLA steel
Published: 2015
Publication type: IOP Conference Series: Material Science and Engineering 75 (2015) 012009 - peer reviewed.

2. Elastic Plastic Fracture Behaviour and effect of Band overload on FCGR of an HSLA Steel
Conference: National Metallurgist's Day 2014- Indian Institute of Metals, Pune, India

3. Band-overload and its effect on FCGR of HSLA steel
Conference: National Conference on Processing & Characterization of Materials 2014 NIT Rourkela, India.

Bio Data

Name S.V.Abhinay

Date of Birth 23.05.1991

Permanent Address

D.no-58-23-30
Baji junction, NAD X Roads
Visakhapatnam
Andhra pradesh
India
Pin: 530027

E-mail ID smrutin9999@gmail.com

Languages Known Telugu, English, Hindi,

Educational Qualifications:

Year	Degree/Certificate	Institution	Marks obtained
2012	Bachelor of Engineering (Metallurgical Engineering)	Andhra University, Andhra Pradesh	CGPA 8.49 out of 10
2008	10+2 (Board of Intermediate Education, Andhra pradesh)	Sri Chaitanya junior college	90.5% 1st Div.
2006	10 (SSC, Andhra pradesh)	Bhashyam public school	89.83 % 1st Div.